Estimating ground precipitation by use of data from the Global Navigation Satellite System (GNSS)
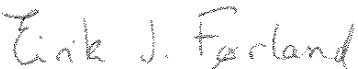
Sofus Linge Lystad

report

Norwegian Meteorological Institute
met.no

Title	Date
Estimating ground precipitation by use of data from the Global Navigation Satellite System (GNSS)	December 22.2011
Section Meteorology and Climate Department	**Report no.** 17/2011
Author(s) **Sofus Linge Lystad**	**Classification** ☒ Free ☐ Restricted
	ISSN 1503-8025
	e-ISSN 1503-8025
Client(s) Telenor, Norwegian Defence, and Norwegian Post and Telecommunication Authority Norwegian Meteorological Institute	**Client's reference**

Abstract
The delay in radio signals from the Global Navigation Satellite System (GNSS) is proportional to the integrated water vapour (IWV) in the atmosphere above the GNSS site. The potential in using GNSS meteorology to determine precipitation intensity at the ground is evaluated. In spite of a rather limited dataset and the fact that high IWV-values does not necessarily imply the release of precipitation, this pilot study shows that there exists a relation between IWV and measured precipitation at the ground.

Keywords
Precipitation intensity, Global Navigation Satellite System (GNSS), integrated water vapour (IWV)

Disciplinary signature	Responsible signature
Eirik J. Førland	*Cecilie Stenersen*
Eirik J. Førland	Cecilie Stenersen

Contents

Introduction

Global Navigation Satellite System (GNSS) radio signals interact with the atmosphere of the earth. The signals slow down and bend, when passing from a GNSS satellite to a ground based receiver, causing a delay of the signals compared to a no atmosphere situation. The delay results in errors when using GNSS signals for positioning. The largest effect is from the ionosphere, but this part is easily subtracted, due to its dispersive (frequency dependent) nature, and the fact that the GNSS satellites emit at two frequencies. The remainder of the delay is due to the neutral atmosphere, near the surface of earth. For geodesists this delay is a noise term, which must be corrected for. For meteorologists it is an important observation, because it contains information on the total water vapour and mass of the atmosphere along the signal path.

The delay caused by the neutral atmosphere is estimated and corrected for, by in the processing of GNSS data fitting the observed GNSS data to a model which includes a delay term, along with many other terms that must be estimated simultaneously. Mapping functions are used to transform from the slant delays at different lower elevation angles to zenith. The mapped delay is called zenith total delay (ZTD). The ZTD estimated can be considered a specially weighted average of the delays toward the individual satellites. The ZTD is typically given as a distance, corresponding to the actual delay multiplied by the speed of light, equal to the apparent extra distance the signals have been traveling.

The ZTD can be divided into two terms. The first term is the zenith hydrostatic or zenith dry delay (ZHD), which is proportional to the pressure at the GNSS receiver site. The second term is the zenith wet delay (ZWD), which is proportional to the integrated water vapour (IWV) above the GNSS site, and which depends weakly on the temperature and humidity profile above the site. The ZHD is of the order 2 m at sea surface, while ZWD varies between 0 and about 0.5 m. The split up requires extra information, e.g. a measured or calculated pressure.

This exercise is to evaluate the potential of GNSS meteorology to determine precipitation at the ground. The main problem is that GNSS meteorology evaluates the vapour content in the atmosphere and as such also "precipitable water", but gives no information whether this water content is released as precipitation reaching the ground.

Possible strategies to evaluate the potential of GNSS meteorology may then be either to look at the minimal values of IWV necessary to release precipitation or to relate the reduction in atmospheric water vapour between two time steps, i.e. IWV, directly to the measured precipitation at the ground.

1. The Global Navigation Satellite System (GNSS)

The GNSS system consists of three parts, the space segment, the control segment and the ground segment. The space segment consists of the satellites, the ground segment of geodetic ground stations with well defined coordinates.

Today two operational global systems exist, NAVAID (also named NAVSTAR) run by USA and GLONASS (Global'naya Navigatsionnaya Sputnikovaya Sistema) run by Russia. In addition the European Union and the European Space Agency (ESA) have decided to launch their own system Galileo, this is today in initial deployment phase, two satellites launched.

System	NAVAID	GLONASS	Galileo
owned/run by	United States	Russia	European Union
Coding	CDMA[1]	FDMA[2]/CDMA	CDMA
Orbital height	20 200 km	19 100 km	23 222 km
Period	12 Hours	11 H 18 m	14 H 6 m
Number of satellites	24 (at least)	24 (30 with CDMA)	22 budgeted
Frequency	1.57542 GHz (L1) 1.22760 GHz (L2)	ca. 1.602 GHz ca. 1.246 GHz	1.164-1.300 GHz 1.559-1.592 GHz
Status	Operational	Operational	In preparation

Table 1.1 The main GNSS systems.
     [1] Code division multiple access
     [2] Frequency division multiple access

There exist also several regional systems and for instance China has indicated the intention to expand their regional system (Beidou) into a global system by 2020. This "Compass" system is proposed to utilize 30 medium earth orbit satellites and 5 geostationary satellites.

Due to the spread spectrum characteristic of the signals, the system provides a large margin of resistance to interference. Each satellite transmits a navigation message containing its orbital elements, clock behavior, system time and status messages. In addition, an almanac is also provided which gives the approximate data for each active satellite. This allows the user set to find all satellites once the first has been acquired.

The control segment (example from NAVAID) consists of one master control station, five monitor stations and ground antennas. The monitor stations passively track each satellite continuously and provide this data to the master control station. The master control station calculates any changes in each satellite's position and timing. These changes are forwarded to the ground antennas and transmitted to each satellite daily. This ensures that each satellite is transmitting accurate information about its orbital path.

The user segment, comprised of both civilian and military users worldwide, acquires signals sent from the GNNS satellites with GPS (Global Positioning System) receivers. The GPS receiver uses these signals to determine where the satellites are located. With this data and information stored internally, the receiver can calculate its own position on earth.

Until 2000, civilian users had to contend with Selective Availability (SA). The United States Department of Defense intentionally introduced random timing errors in NAVSTAR satellite signals to limit the effectiveness of GPS and its potential misuse by adversaries of the United States. These timing errors could affect the accuracy of readings by as much as 100 meters.

With SA removed, a single GPS receiver from any manufacturer can achieve accuracies of approximately 10 meters. To achieve the accuracies needed for higher quality, from one to two meters up to a few centimeters, requires differential correction of the data.

The underlying idea of differential GPS (DGPS) is that any two receivers that are relatively close together will experience similar atmospheric errors. DGPS requires that a GPS receiver be set up on a precisely known location. This GPS receiver is the base or reference station. The base station receiver calculates its position based on satellite signals and compares this location to the known location. The difference is applied to the GPS data recorded by the second GPS receiver, which is known as the roving receiver. The corrected information can be applied to data from the roving receiver in real time in the field using radio signals or through post processing after data capture using special processing software.

As an example from Norway, the reference stations in the SATREF system established and run by the national mapping agency (NMA) at Hønefoss, are the so called CPOS-stations. This system utilizes both NAVSTAR and GLONASS satellites and that gives accuracy in positioning better than 5 cm in horizontal coordinates and 8 cm in the vertical in 95% of time. More or less similar geodetic reference stations are distributed all over Europe.
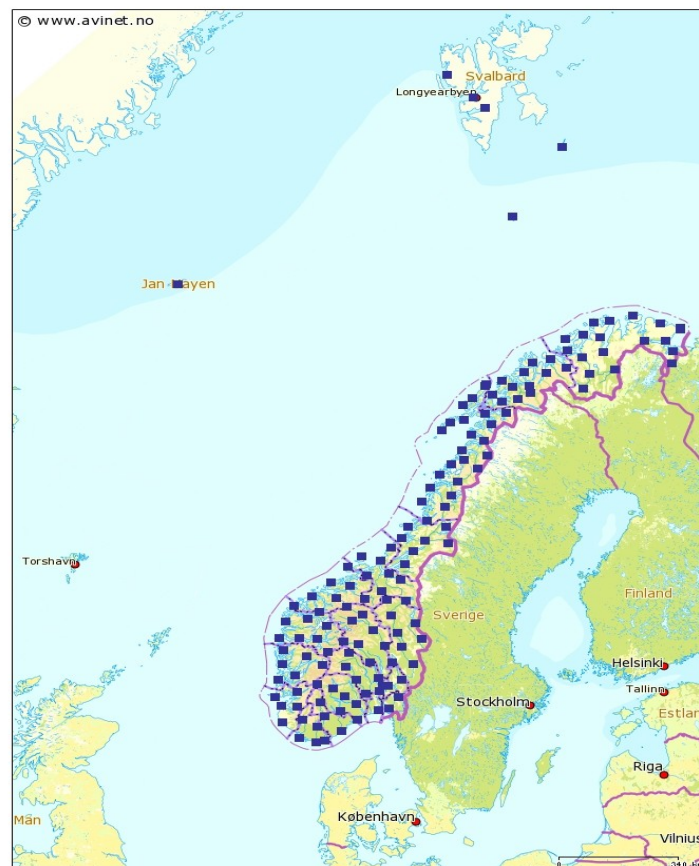

Fig 1.1 Map of the Norwegian CPOS network. Map taken from Norwegian NMA.

In addition to the shown CPOS network in figure 1.1 it exists similar stations on most of the oil platforms in the North Sea. Data from those are collected by the Norwegian NMA in non real time, but in the future they will also be available as part of the ordinary CPOS network.
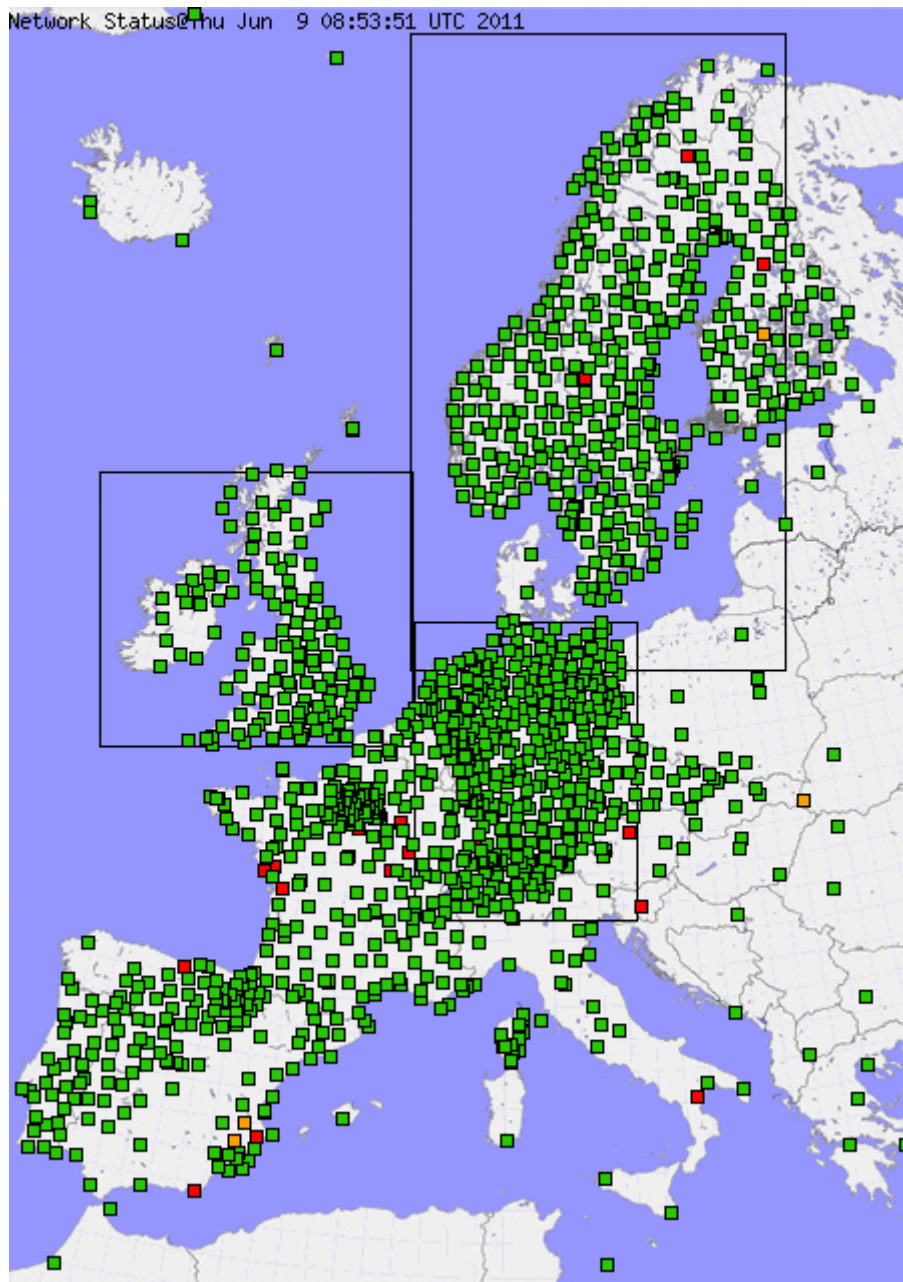
Fig 1.2 Map of the European GNSS ground stations included in the E-GVAP programme. Map by the courtesy of KNMI.

In figure 1.2 is shown the GNSS ground stations used by the different analysis centres (AC's) shown in annex 2. The number of stations is still increasing as agreement with the third party (commercial) stations is done. It is the expectation that The Norwegian Meteorological Institute in the near future can also serve as an analysis centre.

The green dots represent data to the meteorological system early enough to be used in an operational weather forecasting model, red dots represent data coming too late for this purpose. An example of the products from AC's, METO and ROB (see annex 2) is given in

figure 1.3 where ZTD and IWV are shown together with results (D_11) from a numerical weather prediction model (NWP), i.e. HIRLAM.

Fig 1.3 ZTD and IWV from AC's METO and ROB for STAS. Figure from KNMI

The International GNSS Service (IGS) (http://igscb.jpl.nasa.gov/) provides ZTD data of currently more than 300 globally distributed GPS stations. To derive IWV from these data, meteorological information (ground pressure and mean temperature above the station) are needed. Only a limited number of IGS stations are equipped with meteorological ground sensors up to now. Thus, meteorological data for IWV conversion are usually derived from nearby ground meteorological observations and meteorological analyses, global NWP, (ground pressure and mean temperature).

Fig 1.4 Map of the IGS stations, taken from http://igscb.jpl.nasa.gov/network/netindex.html

1.1 The E-GVAP programme.

The work in European GNSS meteorology is organized in a EUMETNET program called E-GVAP (see http://www.egvap.dmi.dk). Most of the material concerning E-GVAP is taken from their homepage or from documents therein.

E-GVAP was set up, in April 2005, to provide its EUMETNET members with European GNSS delay and water vapour estimates for operational meteorology in near real-time.

Currently 13 EUMETNET members are members of E-GVAP-I (Belgium, Croatia, Denmark, Finland, Iceland, Ireland, Norway, Netherlands, France, Sweden, Spain, Switzerland, United Kingdom).

The NRT (near-real time) GNSS delay data contain information about the amount of water vapour above the GNSS sites. Water vapour plays a key role in some of the most important weather phenomena: It is obviously related to precipitation, but also provides about half the energy to the atmosphere (via latent heat release), contributing to atmospheric dynamics, and it is the dominant greenhouse gas. There is a big lack of humidity observations in the meteorological observing system, usage of ground based GNSS data is one means by which to improve on this.

The vast majority of high quality permanent GNSS sites are installed for positioning purposes, by geodetic institutions and private firms. To them the atmospheric delay is a noise term. The core of E-GVAP is a close collaboration between geodesy and meteorology. Raw data from GNSS sites are collected by a number (more than 10) GNSS analysis centre,see annex 2, which process the data to estimate ZTDs (and other parameters). The ZTDs are then forwarded to a dataserver, for distribution to meteorological institutes and for quality control and verification. E-GVAP contributes meteorological data, which can be used to validation GNSS delay estimation, and to improve GNSS positioning in the future.

For the moment the E-GVAP network consists of more than 1500 GNSS sites. Mainly in Europe, but recently processing and distribution of global GNSS data has started, since many E-GVAP members run global NWP models. For the same reason E-GVAP welcomes collaboration with both European and non European institutions, in order to densify the GNSS meteorological observing network.

The exchange of data is now in many cases governed by memorandums of understanding (MoUs). Most recently an MoU was made between EUREF (an inter European body in GNSS geodesy,) and EUMETNET, about access to GNSS data from the so-called EPN sites, which are used to construct the European part of the reference frame of the Earth, to which all the GNSS observations are tied in the processing of the data.

2 Short introduction to GNSS meteorology.

The atmosphere affects microwave transmissions from space in different ways. The waves travel slower than they would in a vacuum and they travel in a curved path instead of in a straight line. Both of these effects are due to a variable index of refraction along the ray path. The influence of the ionosphere will be briefly discussed in a later paragraph. The delay in signal arrival time through the lower atmosphere can be stated in terms of an equivalent increase in travel path length. This excess path length is given by

$$dL = \int_s n(s)ds - L \tag{2.1}$$

where n(s) is the refractive index as a function of position s along the curved ray path S, and L is the straight-line geometrical path length through the atmosphere, that is the path that would occur if the atmosphere was replaced by a vacuum. Equivalently,

$$dL = \int_S (n(s) - 1)ds + (S - L) \tag{2.2}$$

where S is the curved path length. The first term on the right is due to the slowing effect, and the second term is due to bending. The bending term [S - L] is much the smaller, about 1 cm or less, for paths with elevations greater than about 15°. For rays oriented along the zenith, and in the absence of horizontal gradients in n, the ray path is a straight line and the bending term vanishes. Equation (2.2) is often formulated in terms of atmospheric refractivity N, defined by $N = 10^6(n - 1)$, rather than the index of refraction. The refractivity of the atmosphere is a function of its temperature, pressure, and water vapour pressure. A well known relationship is

$$N = 77.6(P/T) + 3.73 \cdot 10^5 (e/T^2) \tag{2.3}$$

Here is P the total atmospheric pressure (hPa), T is the atmospheric temperature (degrees Kelvin), and e is the partial pressure of water vapour (hPa). This expression is considered accurate to about 0.5% under normal atmospheric conditions. In most contexts the first term is much larger than the second. A more accurate formula for refractivity is provided by Thayer [1974]

$$N = k_1(P_d/T)/Z_d + k_2(e/T)/Z_v + k_3(e/T^2)/Z_v \tag{2.4}$$

Where $k_1 = (77.604 \pm 0.014)$ K hPa^{-1} , $k_2 = (64.79 \pm 0.08)$ hPa^{-1} , $k_3 = (3.776 \pm 0.004) 10^5 K^2$ hPa^{-1} , P_d is the partial pressure of dry air (hPa), and Z_d and Z_v are the inverse compressibility constants for dry air and water vapour. Both of these factors, which are corrections for nonideal gas behavior, have nearly constant values that differ from unity by a few parts per thousand and can therefore be assigned the value of one. The uncertainties in the constants of equation (2.4) limit the accuracy with which the refractivity can be computed to about 0.02%.

Saastamoinen [1972] showed that the total atmospheric delay can be partitioned into a large quantity which depends only on surface pressure, called the "hydrostatic delay," and a smaller quantity which is a function of water vapour distribution and is called the "wet delay". The largest contribution to the hydrostatic delay is that of the dry air. Nevertheless, the hydrostatic

delay also includes a significant contribution from water vapour due to the nondipole component of water vapour refractivity. Wet delay is produced solely by atmospheric water vapour (due to the dipole component of its refractivity), though it should be kept in mind that it is not the only delay produced by water vapour.

So just as the refractivity N is divided in a dry and a wet part we can also divide the excess length dL in a "dry" or a hydrostatic part and a "wet" part as

$$ZTD = ZHD + ZWD$$

Where ZTD is the zenith total delay, ZHD is the zenith hydrostatic delay and ZWD is the zenith wet delay, all given in "length units".

Using the previous equation (2.4), ZTD can be expressed in terms of pressure dp as the sum of a hydrostatic part ZHD and the non-hydrostatic part, or the wet part ZWD

$$ZTD = \int_{top}^{ground} (k_1 R_d / g)dp + \int_{top}^{ground} (qR_d((k_2 - k_1\varepsilon) + k_3/T)/g\varepsilon)dp \qquad (2.5)$$

where q is the specific humidity, R_d is the specific constant of dry air, g is the gravitational "constant", T is the temperature and ε is the ratio of the water vapour constant to that of dry air. "top" stands for top of atmosphere.

Solving the integral for ZHD we obtain that it depends by only the surface pressure P_s

$$ZHD = k_1 R_d P_s/g \qquad (2.6)$$

If the barometric pressure is known with accuracy to 1 hPa, ZHD can be estimated with an accuracy of 2.3 mm. The zenith hydrostatic delay has a typical magnitude of about 2.3 m at sea level. If surface pressure measurements are better than 0.3 hPa it is usually possible to predict ZHD to better than 1 mm. Values of ZHD for different pressures at ground level are given in table 2.1:

Pressure (hPa)	900	950	1000	1050	1100
ZHD (m)	2.044388	2.157965	2.271543	2.385120	2.498697

Table 2.1 ZHD for different pressures at sea level.

The zenith wet delay ZWD, can vary from a few millimeters in very arid conditions to more than 350 mm in very humid conditions. It is not possible to predict the wet delay with useful degree of accuracy from surface measurements of pressure, temperature and humidity. Almost all of the wet delay occurs in the troposphere, and most of it occurs in the lower troposphere.

Assuming hydrostatic equilibrium, the ZHD can be calculated as a function of the surface pressure P_s (at GPS antenna height) with the formula of Saastamoinen (1972)

$$ZHD = (2.2768 \pm 0.0005)P_s/f(\varphi, H)$$

with ZHD in mm and P_s in hPa. The term

$$f(\varphi,H)=1-0.00266\cos2\varphi-0.00028H$$

accounts for the dependence of gravity acceleration from latitude φ and surface height above the ellipsoid H (in kilometers).

The wet delay, ZWD, can then be computed as the difference between the total delay, ZTD, and the dry or hydrostatic delay, ZHD.

The ratio between the integrated water vapour IWV or what we may call precipitable water and ZWD is given by a conversion factor Π, (Askne and Nordius 1987).

$$IWV=ZWD\cdot\Pi$$

which depends on the water vapour weighted atmospheric mean temperature T_m.

$$\Pi^{-1}=10^{-6}\rho\, R_v[c_1/T_m+c_2]$$

Here ρ denotes the density of liquid water (10^3 kg m^{-3}) and R_v the specific gas constant of water vapour (461.5 J kg^{-1} K^{-1}). The constants follow from equation (2.4) as

$$c_1=k_3$$

$$c_2=k_2-(M_w/M_d)\,k_1$$

where M_w and M_d is the molar masses of water vapour and dry air respectively

The water vapour weighted mean temperature is defined as

$$T_m=\int(e/T)dz\,/\int(e/T^2)dz$$

and can be calculated from vertical profiles of water vapour pressure e and temperature T, usually derived from NWP analysis fields. Assuming a linear relation with surface temperature it is also possible to approximate T_m from station temperature observations T_s (Bevis et al., 1992).

$$T_m\approx70.2+0.72T_s$$

2.1 Influence of the ionosphere.

The free electrons of the ionosphere, which extends from about 50 to about 1000 km above the Earth's surface, affect the propagation of radio waves. At frequencies above about 30 MHz, radio waves pass through the ionosphere but suffer dispersion. The phase velocities of carrier waves are increased, but the group velocities of modulations superposed on the carrier waves are reduced. The magnitude of phase advance and group delay are similar, the effects differ only in sign. The magnitude of the group delay is, to a good approximation, proportional to the total electron content (TEC) along the path between satellite and receiver and inversely proportional to the square of the carrier frequency.

The TEC varies substantially both in time and space, with extreme values of about 10^{16} and 10^{19} el m $^{-2}$. The TEC is mainly a function of incident solar radiation flux. For example, during the day the ionizing effects of incident solar energy increase the TEC, and at night free electrons tend to recombine with ions, and TEC is reduced. The TEC is affected by a wide range of phenomena including the sunspot cycle, the rotation of the sun, traveling ionospheric disturbances (TIDs), and more rapid ionospheric scintillations, the Earth's magnetic field, season, location, and direction. A typical daily average zenith delay due to the ionosphere is 10 m. The delay can change by an order of magnitude between day and night. TIDs, which are thought to be related to weather patterns, have spatial wavelengths between several hundred and several thousand kilometers and temporal periods between 10 minutes and several hours. They typically cause ~ 10% fluctuations in the total ionospheric delay.

By making measurements at two sufficiently widely spaced frequencies the ionospheric effect can be modeled and largely removed from the observations. It is for this reason that GPS satellites transmit signals on two carrier frequencies: L1 at 1.57542 GHz and L2 at 1.22760 GHz (NAVSTAR) with wavelengths of about 190 and 244 mm, respectively.

A dual-frequency GPS receiver records the differential group delay between the L1 and L2 frequencies, and the total delay at either frequency can be estimated from this observation using a model for ionospheric dispersion. The standard dual-frequency correction ignores third- and higher-order terms in the refractive index of the ionosphere. Nevertheless, it achieves (for elevation angles > 15°) a residual range error (RRE) of less than 30 mm in all but unusual circumstances. The RREs generated by the standard model tend to decrease with increasing elevation angles; at zenith the RRE is almost always less than 10 mm. Because the ZWD normally is estimated at each epoch using observations from four or more satellites, the residual range errors may partially cancel during the computation of the ZWD. More importantly the mapping function used in the computation of the ZWD tends to reduce the influence of large RREs obtained at low elevations. Thus one would expect the ionosphere RREs under normal conditions to induce ZWD errors of less than 10 mm and usually of the order of a few millimeters. Recent improvements in the dual-frequency range correction algorithm, which involve approximate expressions for the higher-order effects, can reduce the residual range error to less than 2 mm at any elevation angle. The suggestion is that when these new algorithms are introduced into GPS processing software, ionospheric error sources contaminating GPS-derived estimates of the ZWD should be reduced by an order of magnitude to ~1 mm or less, except under extraordinary circumstances such as a major magnetic storm.

3. Data sources.

Since the purpose of this report is to evaluate the relation between the integrated water vapour given by the GNSS system and the measured precipitation at ground level, we choose a precipitation station recording every minute Stavanger-Våland and a nearby GNSS station STAS, which is the GNSS name for Stavanger.

The coordinates of the stations are given in table 3.1

	Latitude	Longitude	Height (m)
Stavanger Våland	58.957	5.730	72
STAS	59.01770	5.59862	66.42

Table 3.1 Coordinates of the used stations.

As seen from table 3.1 the location of the stations are not identical and that may be a cause for discrepancies in the different data sets.

Data from STAS are obtained from the data hub of E-GVAP at UK. Met Office and have been through a quality check at Danish Meteorological Institute by the kind courtesy of the E-GVAP programme manager Henrik Vedel.

An example of the data from METO is shown below:

```
2.3478  0.0009  0.0317  4.8000  0.145 2009  1  1  5  0  0 STAS METO  59.01771  5.59862
2.3489  0.0009  0.0328  5.0000  0.145 2009  1  1  5 15  0 STAS METO  59.01771  5.59862
2.3493  0.0009  0.0332  5.1000  0.145 2009  1  1  5 30  0 STAS METO  59.01771  5.59862
2.3505  0.0009  0.0344  5.2000  0.145 2009  1  1  5 45  0 STAS METO  59.01771  5.59862
2.3498  0.0010  0.0337  5.1000  0.161 2009  1  1  5 59  0 STAS METO  59.01771  5.59862
2.3470  0.0006  0.0300  4.6000  0.097 2009  1  1  6  0  0 STAS METO  59.01771  5.59862
2.3464  0.0006  0.0294  4.5000  0.097 2009  1  1  6 15  0 STAS METO  59.01771  5.59862
2.3484  0.0006  0.0314  4.8000  0.097 2009  1  1  6 30  0 STAS METO  59.01771  5.59862
2.3496  0.0007  0.0326  5.0000  0.113 2009  1  1  6 45  0 STAS METO  59.01771  5.59862
2.3498  0.0008  0.0328  5.0000  0.129 2009  1  1  6 59  0 STAS METO  59.01771  5.59862
2.3500  0.0005  0.0321  4.9000  0.081 2009  1  1  7  0  0 STAS METO  59.01771  5.59862
2.3509  0.0005  0.0330  5.0000  0.081 2009  1  1  7 15  0 STAS METO  59.01771  5.59862
2.3524  0.0005  0.0345  5.2000  0.081 2009  1  1  7 30  0 STAS METO  59.01771  5.59862
2.3537  0.0006  0.0358  5.4000  0.097 2009  1  1  7 45  0 STAS METO  59.01771  5.59862
2.3553  0.0007  0.0374  5.7000  0.113 2009  1  1  7 59  0 STAS METO  59.01771  5.59862
```

The first column is the ZTD values; the second column contains estimated error value of the ZTD, both in m. The third column is the computed wet delay or ZWD also in m. IWV or integrated water vapour is in the fourth column with estimated error in the fifth column, both in kg m^{-2}. The next five columns indicate time as year, month, day, hour, minute and second. The next column (the twelfth) is the identification of the GNSS station from the geodetic system, (STAS is here Stavanger). The next column gives name of the AC or the analysing centre, METO is here UK Met Office. The two last columns give for the geodetic station latitude and longitude, respectively.

From the example is removed from the original file one column in the beginning giving the "Julian day" as 14 digit number defined so that the first of January is in the interval [0; 1[that is 1 less than normal so that a normal year ends up with 365 days. This is the information given by METO, some of the other AC's give only the ZTD value. Also some quality flags in the end of each record are removed.

METO processes, as seen, data every quarter of an hour. The other analysis centres keep the processing for each hour. In the future of E-GVAP it is a goal to get 15 minute processing at all centres.

Since the most common is one hour processing we chose 1 hour values of IWV, ZTD and ZWD also precipitation values are given each hour as shown in the example from Stavanger-Våland below:

```
06.01.2009 00:00 0
06.01.2009 01:00 0
06.01.2009 02:00 0
06.01.2009 03:0+0 0
06.01.2009 04:00 0
06.01.2009 05:00 0
06.01.2009 06:00 0
06.01.2009 07:00 0
06.01.2009 08:00 0
06.01.2009 09:00 0
06.01.2009 10:00 0
06.01.2009 11:00 0
06.01.2009 12:00 0
06.01.2009 13:00 1.6
06.01.2009 14:00 4.3
06.01.2009 15:00 4.6
06.01.2009 16:00 3.4
06.01.2009 17:00 0.1
06.01.2009 18:00 0
06.01.2009 19:00 0
06.01.2009 20:00 0
06.01.2009 21:00 0
06.01.2009 22:00 0
06.01.2009 23:00 0
```

An example of precipitation data from Stavanger-Våland.

The different columns yield month, day, year, hour and precipitation value in mm.

Some remark about the precipitation values is appropriate at this point. In parts of April, by some unexplainable reason, Stavanger-Våland did not record minute values of precipitation, but only 12 and 24 hourly sums of the precipitation. That implies no data for April in tables 4.4 and 4.6.

4. Results

As indicated in the introduction we try two strategies; one is to try to determine a limiting value for IWV indicating that precipitation will occur, the other is to try to compare difference in the IWV values before and after a precipitation incident with the measured precipitation at the ground.

From the year 2009 we start with isolating from the precipitation station continuous precipitation events with measured precipitation of roughly 10 mm or more. Precipitation is now integrated to mm per hour. From the identical periods in the GNSS data are obtained for the maximum and minimum values of IWV. Maximum value occurs always in the beginning of each period and the minimum value at the very end of the rain period. The difference in integrated water vapour should then indicate the amount of released water. The mass of water precipitated per unit area is expressed by the depth that it fills in mm and taking into account that the density is 10^3 kg m^{-3}, 1 kg m^{-2} of precipitated water is equivalent to 1 mm. The results of this procedure are given in table 4.4.

If the air had been stationary we could the have expected a rather close relationship between the difference in IWV in kg m^{-2} and the measured ground precipitation in mm. But since for the coastal station Stavanger- Våland nearly all rain events are connected with frontal movements, such a close relationship is not to be expected.

The onset of release of precipitation is inevitable dependent of the amount of water vapour in the atmosphere, but also of the thermal stratification of the atmosphere and last but not least of the stability of the air masses. In addition concepts as "warm" or "cold" clouds would give rise to different mechanisms for release of precipitation. Also the difference between stratiform and cumuliform clouds would give different mechanisms for precipitation.
As mentioned also advective effects play a role, moving fronts or air masses may maintain a high content of water vapour in the atmosphere in spite of falling and measured rain at the ground. That implies that the difference in water vapour in the atmosphere before and after a rain incident would be less than the value converted to mm at the ground.

In tables 4.1, 4.2 and 4.3 is given monthly data surveys for IWV, ZTD and ZWD respectively. In the mean values for all variables we clearly recognizes the seasonal variation caused by the thermal content of the atmosphere, this is also reflected in both the maximum and minimum values of the parameters. We also recognize that the maximum values also indicate precipitation as given in the table 4.4. This is not necessarily the lowest maximum value to insure release of rain, but indicate that such a maximum value" always" should give precipitation regardless of season.

We also recognize the greatest values of the variance for all three parameters in the months August and September, especially for the wet delay ZWD. This may be caused by passing fronts from the North Sea. In these months the sea has maximum heat content and can supply the air with an ample amount of humidity by evaporation, the air is also "warm" so the IWV can reach rather high maximum values.

In table 4.4 is given the selected continuous rain periods with the difference in IWV and measured rain at ground (RR) in mm. Also time span for the rain period with mean rain intensity in mm/hour is given. As expected we find that the IWV difference (in kg/m^{-2} equal to mm) for the most part is less than the ground measured precipitation.

month	mean	variance	maximum	minimum
January	9.24	14.52	22.40	2.30
February	9.19	14.56	21.50	1.60
March	10.21	8.40	18.80	3.60
April	13.75	15.50	23.00	6.50
May	13.29	14.88	23.10	4.90
June	14.17	22.35	27.80	5.50
July	22.57	14.93	34.80	12.40
August	22.91	32.58	38.90	12.80
September	18.85	34.82	43.10	7.00
October	12.89	20.56	25.70	5.30
November	13.58	22.50	29.60	3.70
December	8.67	13.74	18.00	1.30

Table 4.1 Integrated water vapour in kg/m^2 for Stavanger 2009.

month	mean	variance	maximum	minimum
January	2.3293	0.0012	2.4042	2.2520
February	2.3422	0.0015	2.4349	2.2525
March	2.3375	0.0010	2.4138	2.2713
April	2.3823	0.0005	2.4294	2.3259
May	2.3790	0.0007	2.4574	2.3078
June	2.3843	0.0014	2.4802	2.3293
July	2.4150	0.0006	2.4860	2.3318
August	2.4279	0.0016	2.5474	2.3383
September	2.4142	0.0015	2.5505	2.3260
October	2.3751	0.0010	2.4865	2.3025
November	2.3387	0.0012	2.4413	2.2731
December	2.3341	0.0014	2.4186	2.2671

Table 4.2 Zenit total delay in m for Stavanger 2009.

month	mean	variance	maximum	minimum
January	0.0601	0.0006	0.1444	0.0150
February	0.0602	0.0006	0.1391	0.0110
March	0.0663	0.0003	0.1215	0.0237
April	0.0883	0.0006	0.1455	0.0416
May	0.0850	0.0006	0.1478	0.0320
June	0.0900	0.0009	0.1745	0.0351
July	0.1424	0.0006	0.2195	0.0785
August	0.1446	0.0013	0.2431	0.0817
September	0.1198	0.0014	0.2718	0.0454
October	0.0830	0.0008	0.1654	0.0344
November	0.0875	0.0009	0.1897	0.0242
December	0.0565	0.0006	0.1161	0.0086

Table 4.3 Zenit wet delay in m for Stavanger 2009.

.

Day/month	IWV (kg/m^2)			Sum RR (mm)	Time span (Hours)	RR mean pr H (mm)
	max	min	difference			
6/1	13.8	7.5	6.3	14.0	7	2.0
8/1	14.3	10.2	4.1	7.3	15	0.5
10-11/1	22.4	15.9	6.5	41.9	36	1.2
18/1	12.9	9.9	3.0	13.2	13	1.0
21-22/2	21.5	9.5	12.0	41.2	30	1.3
26/2	11.9	9.2	3.7	7.0	9	0.8
6/3	14.6	8.5	6.1	14.5	26	0.6
8/3	16.0	7.0	9.0	10.0	5	2.0
12-13/3	13.2	8.3	4.9	8.9	18	0.5
7/5	21.3	11.0	10.3	11.2	8	1.4
26/5	22.9	10.4	12.5	18.5	12	1.5
17/6	24.1	13.6	10.5	13.7	13	1.1
6/7	25.4	23.1	2.3	9.9	3	3.3
13/7	28.6	21.4	7.2	7.4	10	0.7
18-19/7	34.8	21.1	13.7	15.6	15	1.0
21/7	21.3	19.5	1.8	9.3	4	2.3
25/7	24.6	20.6	4.0	24.5	12	2.0
27/7	28.5	19.0	9.5	18.1	12	1.5
30-31/7	28.0	13.9	14.1	43.7	27	1.6
14-15/8	37.5	18.0	19.5	27.5	24	1.2
16/8	25.9	19.5	6.4	18.0	18	1.0
27/8	32.1	22.4	9.7	14.1	14	1.0
29-30/8	21.1	14.9	6.2	38.6	27	1.4
27-28/9	29.2	14.4	14.8	11.1	13	0.9
28/10	22.0	19.9	2.1	15.1	15	1.0
2/11	18.7	11.6	7.1	17.6	21	0.8
14/11	23.9	10.1	13.8	23.5	27	0.9
22/11	24.9	13.0	11.9	20.1	12	1.7
6/12	16.3	9.3	5.0	9.6	17	0.6
19/12	11.8	7.7	4.1	47.3	22	2.5

Table 4.4 Selected continuous rain periods for Stavanger-Våland for the year 2009 with corresponding IWV values from STAS.

From table 4.4 we recognize three peculiarities, first the 27-28/9 as the only one where the difference in IWV is greater than the measured precipitation, sum RR. A possible reason is that some part of the reduction in IWV has transformed into cloud water. The two other cases are the two shortest rain periods as 6/7 (3 hours) and 21/7 (4 hours). The difference in IWV and sum RR is also rather great. Looking at the course of IWV for these two periods we find a greater value of IWV some hours before the onset of precipitation. The "corrected" values are given in table 4.5.

Day/month	IWV (kg/m^2)			Sum RR (mm)	Time span (Hours)	RR mean pr H (mm)
	max	min	difference			
6/7	30.1	23.1	7.6	9.9	3	3.3
21/7	22.5	19.5	3.0	9.3	4	2.3

Table 4.5 "Corrected" maximum values for IWV

Combining table 4.1 (monthly maximum IWV) with table 4.4 (maximum IWV in the selected rain periods, IWVrain) and also mean maximum IWV for all precipitation periods in the given month, IWVrainm we get table 4.6. Here we clearly see the relation between the monthly maximum values of IWV and the IWV in the beginning of substantial rain periods.

	Jan.	Feb.	Mar.	Apr.	May	Jun.	Jul.	Aug.	Sep.	Oct.	Nov.	Des.
IWVmax	22.4	21.5	18.8	23.0	23.1	27.8	34.8	38.9	43.1	25.7	29.6	18.0
IWVrain	22.4	21.5	16.0	----	22.9	24.1	34.8	37.5	29.2	22.0	24.9	16.3
IWVrainm	15.8	16.7	14.6	----	19.1	24.1	27.3	29.1	29.2	22.0	22.5	14.0

Table 4.6 Monthly maximum IWV (IWVmax) and maximum IWV in the onset of rain periods (IWVrain) and mean maximum for all periods in given month (IWVrainm).

As mentioned the precipitation values for April are missing. In spite of rather few data we may try to evaluate a linear relationship between those two variables and get the relation as

$$IWVrain = 0.72 \; IWVmax + 4.78$$

The correlation is $r^2 = 0.77$. The plot of the data is shown in figure 4.1
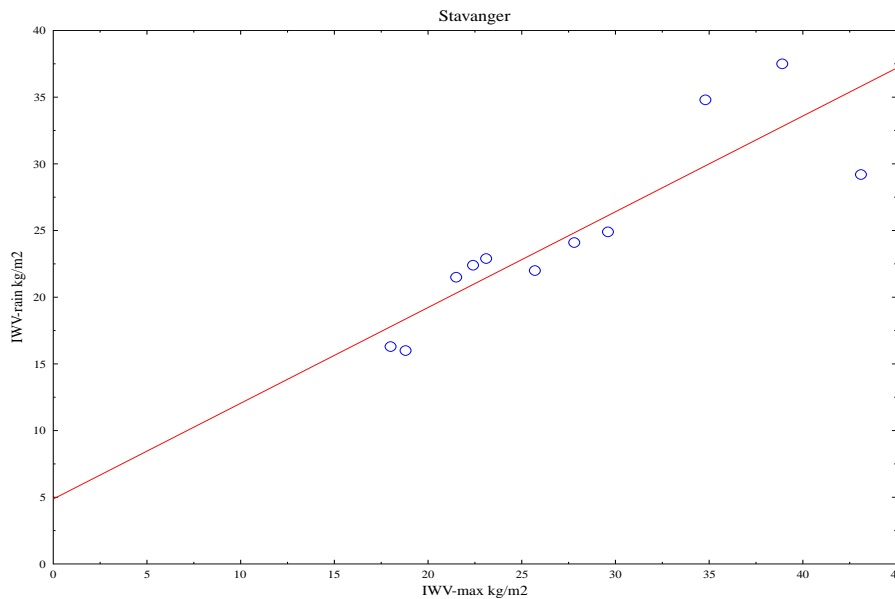
Figure 4.1 Monthly maximum IWV and maximum IWV in the onset of rain periods

However, September, date 8, is a good example of that a high value of integrated water vapour not necessarily gives rise to substantial precipitation at ground. At hour 17 the IWV is 43.1 kg/m^2, first recorded precipitation is at 19 hour with 0.6 mm, IWV is now 38.6 kg/m^2. Then we have 3 hours without precipitation, then 2 hours with a precipitation sum of 1.8 mm. Again 3 hours without precipitation followed by 2 hours with a precipitation sum of 0.4 mm. Now IWV has diminished to 17.6 Kg/m^2. That is in total 2.8 mm intermittent precipitation distributed over 11 hours with a total difference in IWV of 25.5 kg/m^2. The weather situation is shown in the following figure.
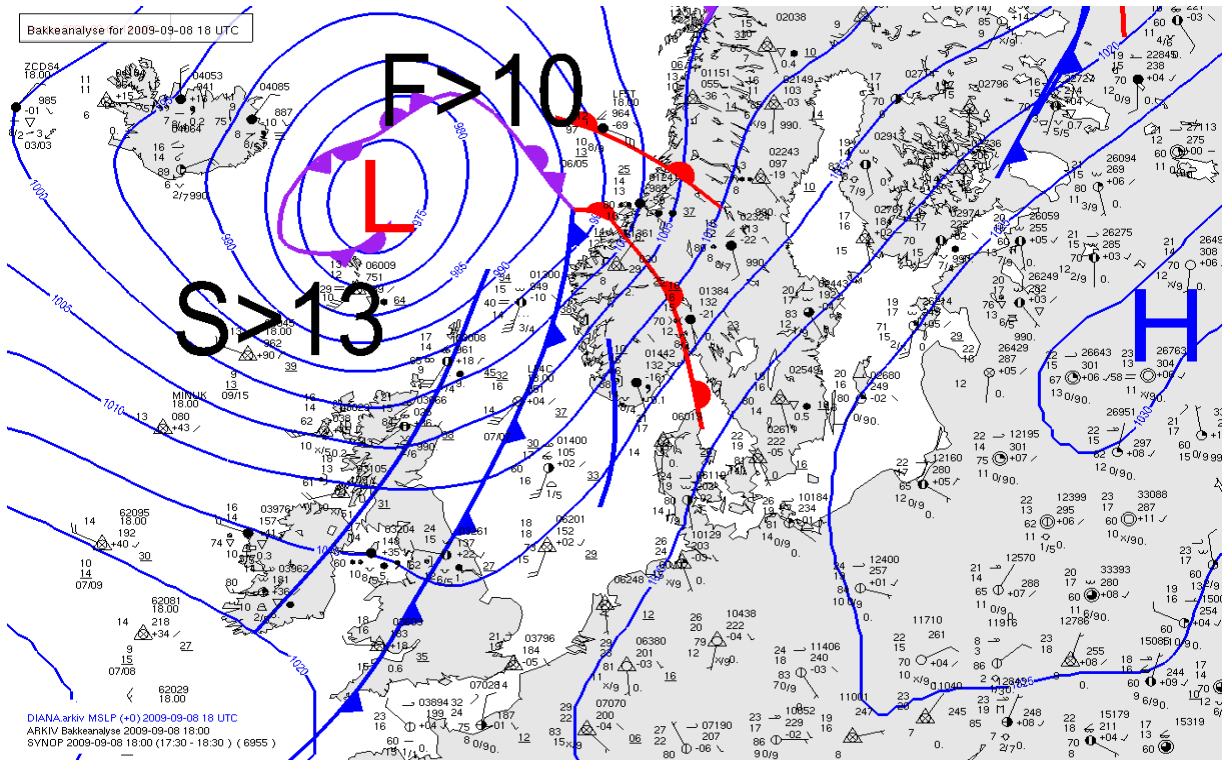
Figure 4.2 Weather map (analysis) of 8/9 2009 at hour 18 UTC.

We see that Stavanger now is in the warm sector of the cyclone. Here is the temperature high enough to maintain a high vapour content, and in the theory no substantial precipitation should occur in the warm sector, which is what we find more or less.

We can also try the relation between IWV and the mean maximum values for the on set of rain in each month and get
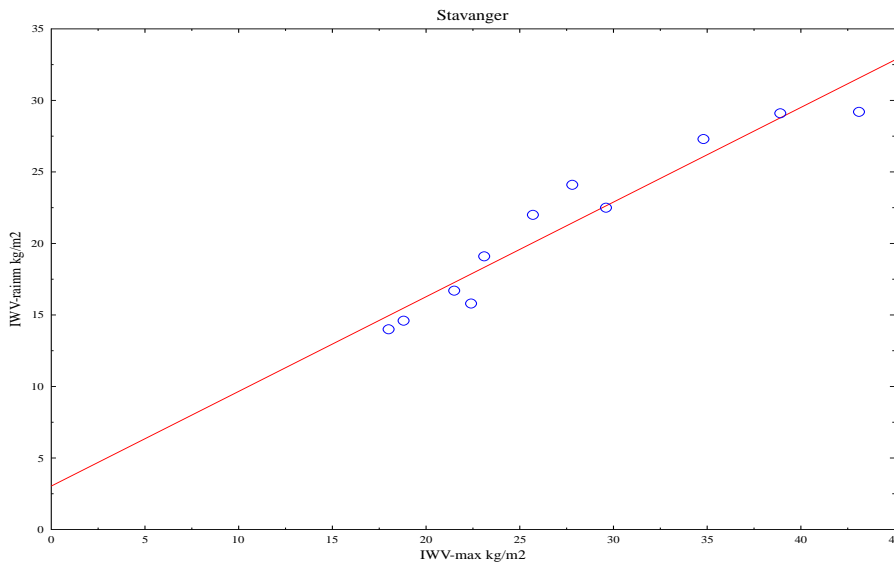

Figure 4.3 Monthly maximum IWV and mean maximum IWV in the onset of rain periods

The linear regression equation is

$$IWVrainm = 0.66 \, IWVmax + 3.04$$

The correlation is $r^2 = 0.92$

A picture of the course of IWV and precipitation for one of the "corrected" periods is shown in figure 4.4
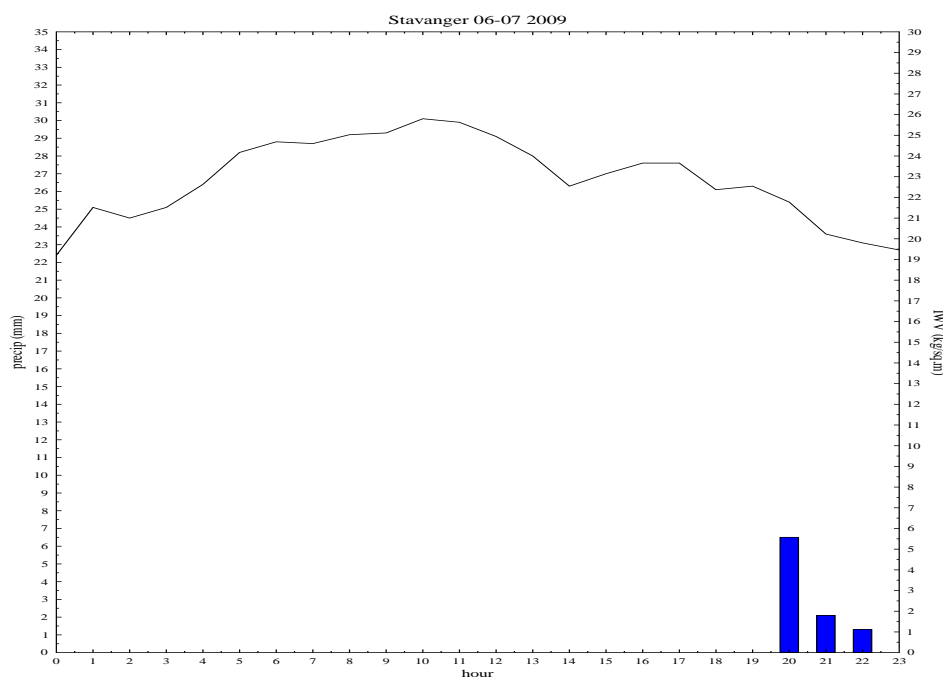
Figure 4.4 IWV and precipitation from 6/7 from Stavanger

To have a closer look at some of the precipitation incidents and the general weather situation we use as examples the dates 18-19/7 and 27-28/9 with precipitation values of 15.6 mm and 11.1 mm respectively. The time spans for the rain periods are 15 hours and 13 hours. In figures 4.5 and 4.7 are shown the weather situation as analysis maps for given hours. In figures 4.6 and 4.8 are shown the hourly precipitation together with the course of IWV.

In both cases we identify the precipitation as frontal precipitation. In July we have an occluded front over Stavanger with high, rather constant values of IWV for several hours. We also notice the diminishing values of precipitation together with the reduction in the values of the integrated water vapour.
In September we have a passing cold front with a pronounced reduction in IWV, this is also, as mentioned previously, the only case where the difference in IWV is greater than the measured precipitation at the ground. Recognizing the rather "bi-modal" behavior of the course of IWV the total period of 13 hours could have been cut in two parts, but between the two pronounced rain periods there are small amounts of precipitation in every hour.
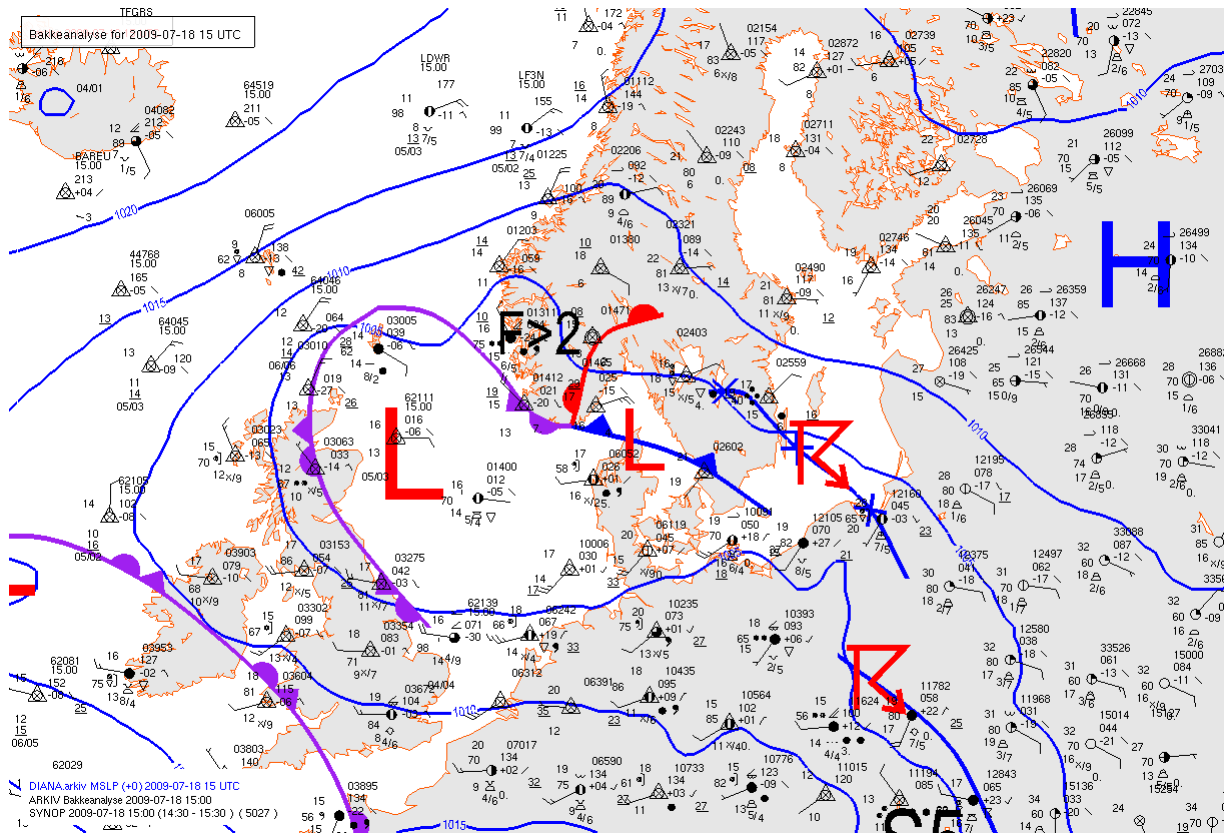
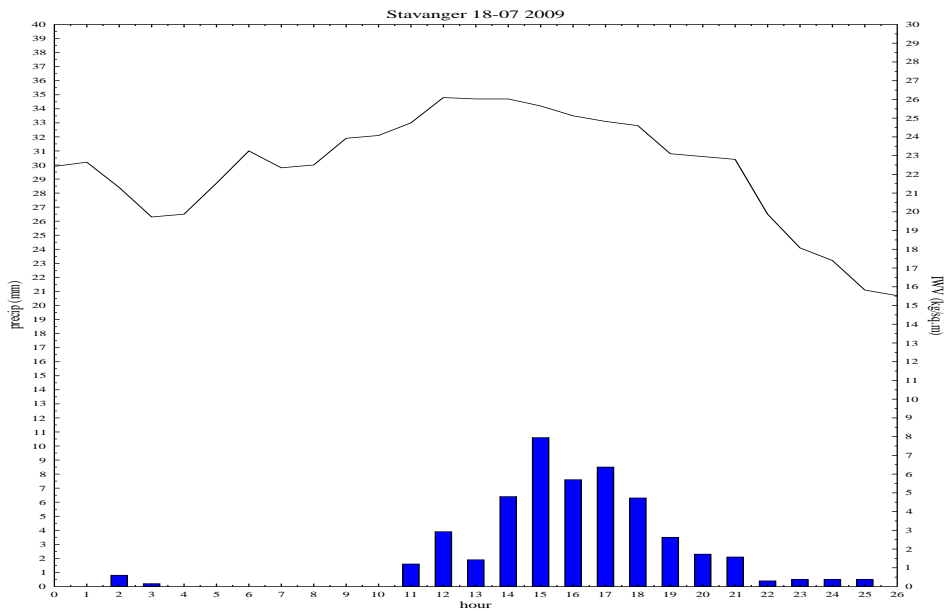Figure 4.5 Weather map (analysis) of 18/7 2009 at hour 15 UTC.

Figure 4.6 Hourly precipitation and the course of IWV of the 18/7
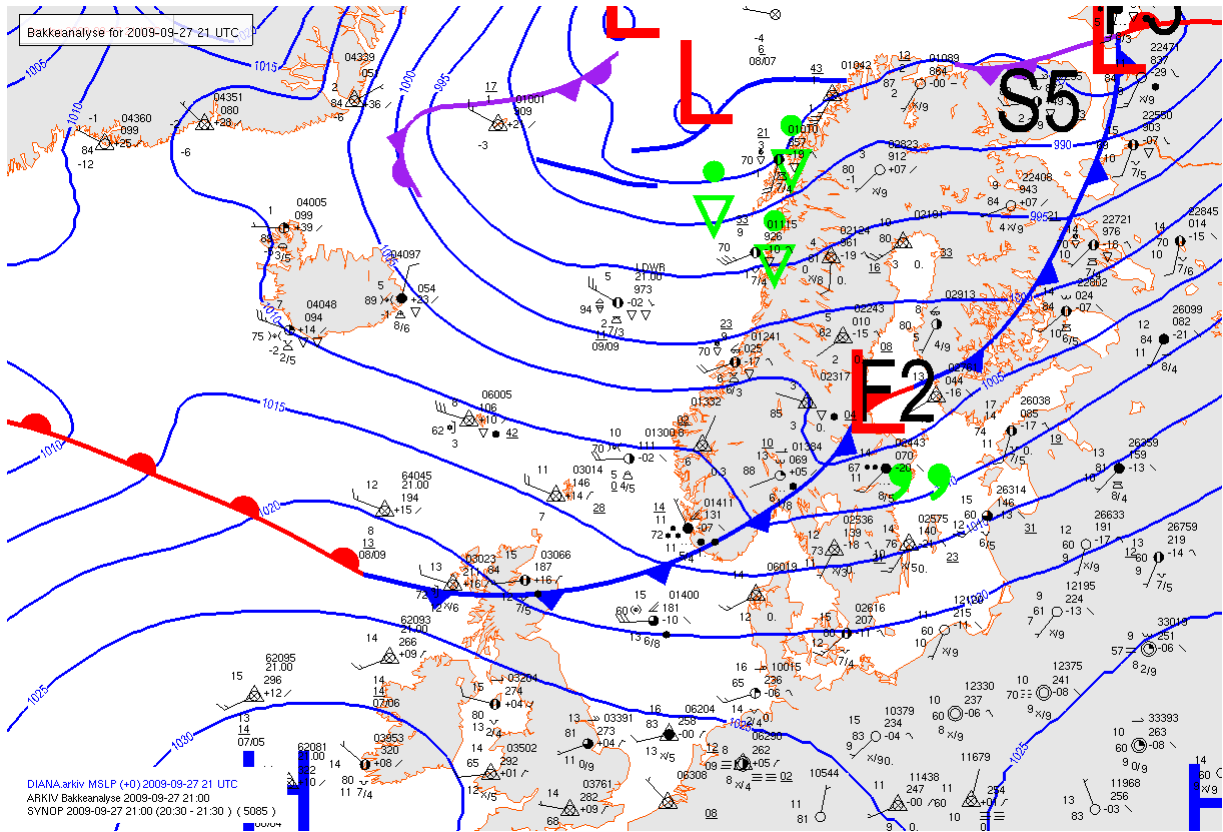
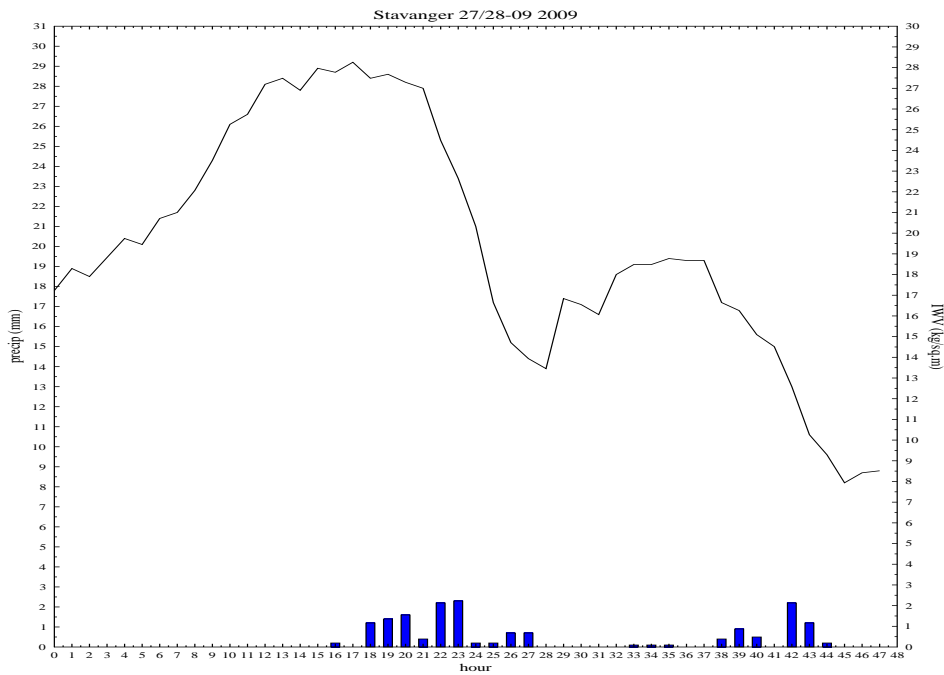Figure 4.7 Weather map (analysis) of 27/9 2009 at hour 21 UTC.

Figure 4.8 Hourly precipitation and the course of IWV of the 27-28/9

A really nice example of the relationship of reduction of integrated water vapour and ground measured precipitation is from 30-31/7.
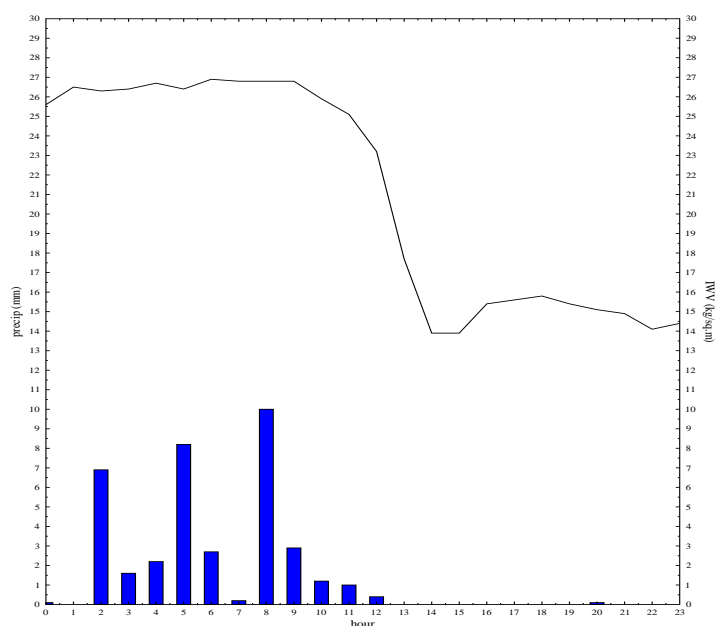

Figure 4.9 Hourly precipitation and the course of IWV of the 30-31/7

In spite of a rather sparse data material, it is tempting to try to get some sort of relationship between the difference in integrated water vapour and measured precipitation. Based on the data from table 2.4 we plot ΔIWV in kgm^{-2} and precipitation in mm in the following figure.
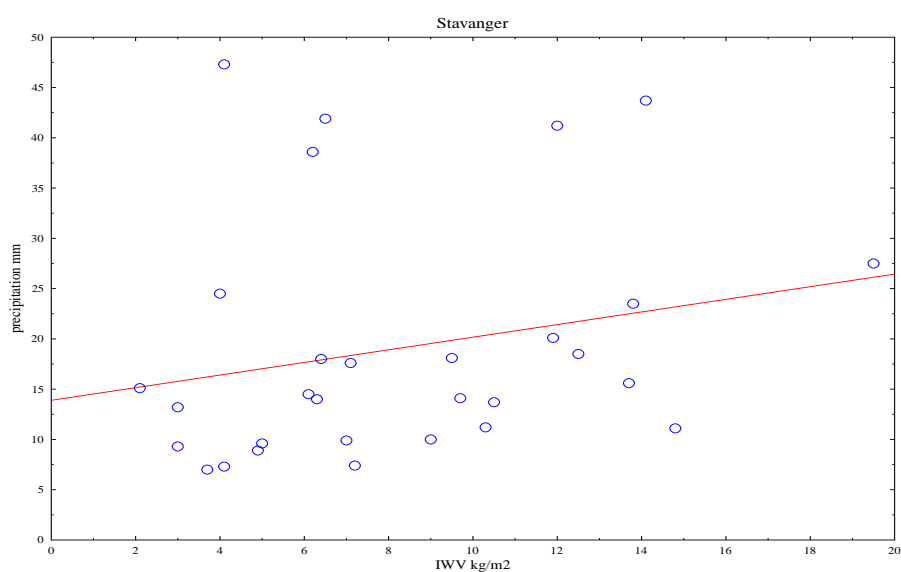

Figure 4.10 Relationship between ΔIWV and measured precipitation, all cases.

We find considerable spread in the data and the correlation is very low $r^2 = 0.05$. The equation for the shown linear relationship is:

$$RR = 0.63 \ \Delta IWV + 13.89$$

We recognize immediately two distinct groups in the data, one group of 5 members with precipitation values around 40 mm and another group with precipitation values less than 30 mm, a maximum value of 27.5 mm. The last group consists of 25 members. A plot of this last group is given in figure 4.11
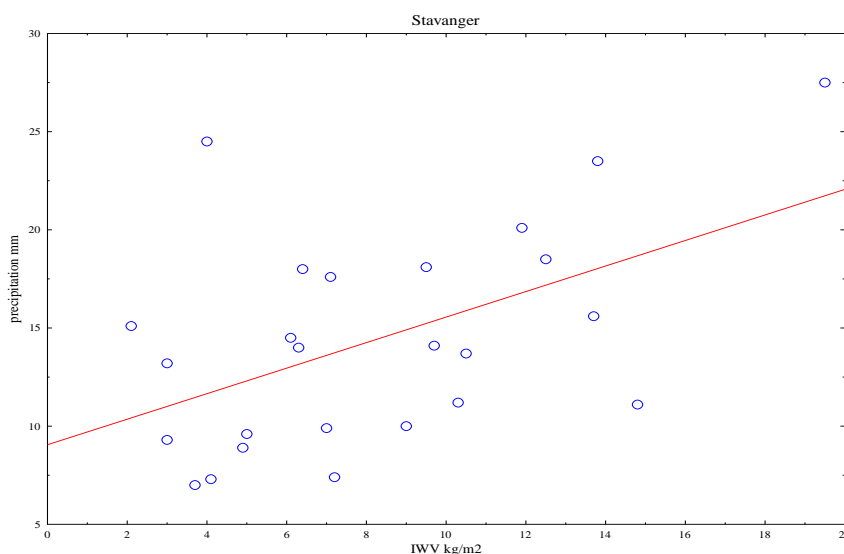

Figure 4.11 Relationship between ΔIWV and measured precipitation, precipitation less than 30 mm.

We find here a small improvement of the correlation, $r^2 = 0.26$ with a similar linear relation as

$$RR = 0.65 \ \Delta IWV + 9.05$$

It is interesting to notice that the regression coefficient of ΔIWV is nearly the same in these two cases.

The group of the great precipitation values is so small that a regression is in vain.

The five periods are recognized by moderate intensities from 1.2 mm/hour to 2.5 mm/hour. Time span in hours is from 22 hours to 36 hours. The time in the year is from January, February, July, August and December. This represent precipitation from frontal systems as shown in figures 4.3 and 4.5, that may release rather great amounts of water for long periods, that is with moderate intensities, but the integrated water vapour may have a great value for a long period.

5. Conclusion

In spite of rather few data (periods with substantial precipitation) and the fact that high values of atmospheric integrated water vapour does not necessarily imply the release of precipitation, we have shown that there exists a relation between IWV and the ground measured precipitation.

The use of the difference in integrated water vapour before and after a precipitation incident is not dependent of the season (e.g. atmospheric thermal content and stability) and should as such be the best indicator among the data from the GNSS system. The difference in kg/m^2 is also directly comparable to the precipitation amount (in millimeters) measured at ground.

This study is based on a very limited set of data. More data and more elaborated analyses could strengthen the relationships between rainfall rates and data from the GNSS system.

Use of the 15 minutes data, (it is the plan within E-GVAP that all analyzing centres should start with this procedure) would be more in line with the concept "rain rate on minute basis". Use of the slant path values, not only the zenith values, could give a better understanding of the three dimensional distribution of water vapour in the atmosphere, this is also a forthcoming task within E-GVAP. Using this in relation to volume data from radar could be fruitful.

If robust relations between IWV and rainfall rates are established, data from the GNSS system could be used to indicate potential rainfall rates for each calendar month for station networks as shown in section 1. However, the uncertainties in these estimates so far are probably too large for estimating rainfall rates with accuracy useful for exact dimensioning purposes.

An alternative strategy might be to study whether the Zenith Wet Delay (which is proportional to the integrated water vapour above the GNSS-site) has closer links to telecommunication conditions than the precipitation amount (i.e. rainfall intensity) reaching the ground.

References

Askne, J., and H. Nordius, (1987) Estimation of tropospheric delay for microwaves from surface weather data,
Radio Sci., 22, 379-386

Bevis M, Businger S, Herring T, Rocken C, Anthes R, Ware R (1992) GPS meteorology: Remote sensing of atmospheric water vapour using the Global Positioning System.
J Geophys Res 97: 15,787-15,801

Saastamoinen, J., Atmospheric correction for the troposphere and stratosphere in radio ranging of satellites, in The Use of Artificial Satellites for Geodesy, Geophys. Monogr. Ser. 15 (S.W. Henriksen et al.,eds.), AGU, Washington, D.C., pp.247-251, 1972.

Thayer, D. (1974): An improved equation for the radio refractive index of air,
Radio Sci**.,** 9, 803-807

Annex 1

Acronyms

AC	Analyzing centre
CDMA	Code division multiple access
CPOS	GNSS ground station in the SATREF system
DGPS	Differential GPS
EIG	Economic Interest Group
E-GVAP	The EUMETNET EIG GNSS water vapour programme
ESA	European Space Agency
EPN	EUREF Permanent Network, a GPS network in Europe
EUCOS	EUMETNET Composite Observing System
EUMETNET	Network grouping 26 European National Meteorological Services
EUREF	European Reference Frame, IAG reference frame sub-commission for Europe
FDMA	Frequency division multiple access
Galileo	Global Positioning System (Europe)
GLONASS	Russian pendent to GPS
GNSS	Global Navigation Satellite System (Generic: GPS, GLONASS, Galileo)
GPS	Global Positioning System (USA)
GTS	Global Telecommunication System
HIRLAM	High Resolution Limited Area Model (NWP)
IAG	International Association of Geodesy
IGS	International GNSS Service
IWV	Integrated water vapour
KNMI	Royal Meteorological Institute of the Netherlands
METO	UK.Met.Office analyzing centre
NAVAID	Navigation Aid, systems as Omega, Loran-C and NAVSTAR
NAVSTAR	USA pendent to GPS
NMA	National Mapping Agency
NMS	National Meteorological Service
NRT	Near-real time
NWP	Numerical weather prediction
ROB	Royal Observatory of Belgium
RRE	Residual range error
SA	Selective Availability
SATREF	Satellite Reference, Norwegian NMA infrastructure for GNSS
TEC	Total electron content
TID	Traveling ionospheric disturbances
WMO	World Meteorological Organisation
ZTD	Zenith total delay (and zenith tropospheric delay, two names for the same property)
ZWD	Zenith wet delay

Annex 2

Analysis centres contributing NRT GNSS delays to E-GVAP

AC Name	Name of organisation	Links
ASI	e-geos/Telespazio, Italy	ASI_ ASIC
BKG	Federal Agency for Cartography & Geodesy, Germany	BKG_ BKGH
GFZ	Helmholz Centre Potsdam GFZ German Reseach Centre for Geosciences	GFZ_
GOP	Geodetic Observatory Pecny Czech Republic	Home GOP1 GOP2 GOPG GOPX
IES	Institute of Engineering, Surveying and Space Geodesy, Univ. of Nottingham, UK	IES2
IGE	Instituto Geografico National, Spain	IGE_ IGE2
IRE	Met Éireann, Rep. Ireland	IRE2
KNMI	Royal Meteorological Inst. of the Netherlands	KNMI KNM1 KNM2
LPT	SwissTopo	Agnes network LPT_ LPTR
METO	UK Metoffice	METO METG
NGAA	Chalmers Tecnical University and Swedish Meteorological and Hydrological Inst	NGAA
SGN	Institut Geographique National, France	SGN_ SGN1
ROB	Royal Observatory of Belgium	EUREF Network ROB_